Harmonic Order Tracking Analysis: a Novel Method for Fault Diagnosis in Induction Machines

A. Sapena-Baño, M. Pineda-Sanchez, *Member, IEEE,* R. Puche-Panadero, *Member, IEEE,* J. Perez-Cruz, *Member, IEEE,* J. Roger-Folch, *Member, IEEE,* M. Riera-Guasp, *Senior Member, IEEE,* and J. Martinez-Roman.

***Abstract*—The diagnosis of induction machines using the Fourier transform relies on tracking the frequency signature of each type of fault in the current's spectrum. But this signature depends on the machine's slip and the supply frequency, so it must be recomputed for each working condition, by trained personnel or by diagnostic software. Besides, sampling the current at high rates during long times is needed to achieve a good spectral resolution, which requires a large memory space to store and process the current spectra.**

In this paper, a novel approach is proposed to solve both problems. It is based on the fact that each type of fault generates a series of harmonics in the current's spectrum, whose frequencies are multiples of a characteristic main fault frequency. The tracking analysis of the fault components using the harmonic order (defined as the frequency in per unit of the main fault frequency) as independent variable, instead of the frequency, generates a unique fault signature, which is the same for any working condition. Besides, this signature can be concentrated in just a very small set of values, the amplitudes of the components with integer harmonic order. This new approach is introduced theoretically and validated experimentally.

***Index Terms*—Induction machines, fault diagnosis, Hilbert transforms, Fourier transforms, condition monitoring, motor-current signature analysis, broken rotor bar detection, harmonic order tracking, signal processing.**

I. Introduction

INDUCTION motors (IMs) condition monitoring plays a vital role in assuring the continuity of modern industrial processes, where IMs are a key component, avoiding costly breakdowns. Motor current signature analysis (MCSA) is the dominant diagnostic method in the area of induction machines fault diagnosis, as stated in [1], due to its low requirements of hardware and software. Just a current sensor is needed to acquire the current signal, and a simple FFT is needed to obtain the current's spectrum. Besides, there is a huge amount of theoretical studies that establish the frequency signature of each fault, and also an extensive industrial experience that has allowed to establish practical diagnostic fault thresholds. This previous knowledge is an important advantage of MCSA, which helps to avoid false positive diagnostics (unneeded and costly interruptions of the service), and false negative diagnostics (which can lead to the machine destruction, besides process interruptions).

MCSA relies on the detection in the current's spectrum of the frequency signatures that have been derived analytically for each type of fault [2]. In particular, rotor asymmetries (such as broken bar faults, broken end rings, high resistance connections, etc.) can be detected through the presence in the current's spectrum of fault harmonics given by [3]

$$f_{\text{asym}} = f_1 + 2ksf_1 \quad k = \pm 1, \pm 2, \pm 3 \ldots, \tag{1}$$

where f_1 is the supply frequency and s is the machine per-unit slip. For the diagnosis of rotor asymmetries, the most used harmonics from (1) are those corresponding to the lowest harmonic order ($k = \pm 1$). These are known as the lower sideband harmonic (LSH) and the upper sideband harmonic (USH), and their frequencies are given by

$$f_{\text{LSH}} = f_1 - 2sf_1 = f_1(1 - 2s), \tag{2}$$

$$f_{\text{USH}} = f_1 + 2sf_1 = f_1(1 + 2s). \tag{3}$$

Furthermore, as [4] states, an effective diagnostic index can be retrieved by summing the amplitudes of these two sideband components in the current spectrum.

Mixed eccentricity faults generate harmonics with frequencies given by [5]

$$f_{\text{ME}} = f_1 + kf_{\text{r}} \quad k = \pm 1, \pm 2, \pm 3 \ldots, \tag{4}$$

where f_{r} is the mechanical rotation frequency of the rotor.

Bearings' cyclic faults generate harmonics with frequencies given by [6], [7]

$$f_{\text{b\_o}} = f_1 + k\ 0.4N_{\text{b}}f_{\text{r}} \quad k = \pm 1, \pm 2, \pm 3 \ldots, \tag{5}$$

for the case of a point defect in the outer race, or

$$f_{\text{b\_i}} = f_1 + k\ 0.6N_{\text{b}}f_{\text{r}} \quad k = \pm 1, \pm 2, \pm 3 \ldots, \tag{6}$$

if the defect is located in the inner race, where N_{b} is the number of bearing balls. Equations (5) and (6) are valid for N_{b} between 6 and 9.

Frequency signatures for other types of faults, such as stator interturn faults [8], can be found in the technical literature. Besides, in the case of mixed faults, as the simultaneous presence of static eccentricity and broken bars presented in [9], additional fault harmonics may appear in the stator current.

As it can be seen in equations (1) to (6), to identify if the frequency of a spectral line in the spectrum corresponds to

This work was supported by the Spanish "Ministerio de Ciencia e Innovación" in the framework of the "Programa Nacional de proyectos de Investigación Fundamental" (project reference DPI2011-23740).

The authors are with the Department of Electrical Engineering, Universitat Politècnica de València, Camino de Vera s/n, 46022, Valencia, Spain. E-mails: ansaba2@upvnet.upv.es, mpineda@die.upv.es, rupucpa@die.upv.es, juperez@die.upv.es, jroger@die.upv.es, mriera@die.upv.es, jmroman@die.upv.es.

a given fault, it is necessary to have an accurate information about the supply frequency f_1 , and also about the machine speed (to compute the slip s or f_r). This information is not stored in the spectrum itself, so when performing the spectrum analysis in the search of a specific fault signature, the supply frequency and the slip information must be retrieved, and the frequency of the suspected faults must be computed with the corresponding expressions (1) to (6). This analysis requires a trained technician [10], or, if automated, advanced artificial intelligence systems, such as neural networks [11], support vector machines [12] or fuzzy systems [13].

Another approach to improve the reliability of the diagnostic process is to concentrate the effort not in adding more computational power to the interpretation of the spectrum, but in condensing the spectrum information about the fault in simple indicators that properly highlight the fault signature, as Filippetti [10] suggests. In the case of faults where the characteristic sideband frequencies are separated from the supply component by multiples of the rotational frequency of the machine, such as in (4) to (6), several works have proposed the so called angular order tracking analysis (OT). Among its many variants, recent proposals are the Vold-Kalman filtering order tracking (VKF-OT) method [14], the angular domain order tracking method (AD-OT) [15], or the equal phase sampling method (ESPM) [16]. To perform an OT analysis of the machine, the current must be either sampled at constant angular displacements, triggered by position sensors (which requires a complex data acquisition equipment), or sampled in the time domain at a very high sampling rate, followed by a time domain to angular domain resampling process [17]. In this way, the fault harmonics appear at integer multiples of the so called angular order, which facilitates the analysis of the spectrum. The method proposed in this paper, the harmonic order tracking analysis (HOTA), presents several new contributions in this context. First, using the existing OT methods cited before, the current signal must be resampled prior to its frequency analysis [14]–[17], but, as [17] states, the spatial sampling frequency is limited by the temporal sampling frequency and the maximum expected velocity of the spatial component. Instead, with the proposed HOTA approach the current signal is not resampled. Second, the OT technique cannot be applied to faults whose characteristic frequency is not a multiple of the rotational frequency, so it cannot be used to detect rotor asymmetry faults, which depend on the machine's slip (1). Instead, the proposed HOTA approach locates the fault harmonics at multiples of their integer order, and is valid for the detection of fault harmonics whose frequency is proportional to the machine's slip, including rotor asymmetry faults such as broken bars. Finally, the HOTA approach is able to generate a unique fault signature, the same for different load and supply conditions, which simplifies the analysis of the spectrum by trained personnel or automated diagnostic systems; and the diagnostic results can be condensed in a very low number of data values, which makes this technique especially well suited for storing or transmitting continuously updated information about the machine's condition.

Following the suggestion of Filippetti [10], the method proposed in this paper rearranges the information of the spectrum so that it highlights the presence/absence of a given fault in a simple and clear way. This method stems from the observation that in (1) to (6) (as in any other theoretical expression of IM fault's frequency signature), there is a common component: the integer order k of the harmonic. In this paper it is shown that if the current's spectrum is obtained using this harmonic order as independent variable, instead of the frequency, then the machine condition can be very easily assessed, either by maintenance personnel or by automatic detection systems.

Additionally, only the amplitudes of the components with integer harmonic orders are needed to perform the diagnosis of the motor, so an extremely reduced spectrum, containing just these values, can be used for diagnostic purposes. This can be a crucial point, for example, in the case of embedded devices operating in real time [18], such as DSPs [19], [20], FPGAs [13], portable devices [21], small wireless sensors [11], [22], low cost processors [23], energy-constrained sensor modules [24], or remote diagnostic systems. Instead of storing, analysing and/or transmitting the whole current's spectrum, with thousands of points, an extremely reduced spectrum, with just the amplitudes of the components with integer harmonic orders (only a few points) suffices in the proposed method for performing the diagnosis of the motor.

The structure of this paper is as follows. In Section II the proposed method is theoretically explained. In Section III, it is experimentally validated in a laboratory test rig using a commercial motor with broken bar faults, working under a wide variety of supply frequencies and loads. Finally, Section IV presents the conclusions of this work.

II. Harmonic Order Tracking Analysis of Induction Machines Faults

The method proposed in this paper for the diagnosis of induction machines, the harmonic order tracking analysis, relies on the fact that in (1), (4), (5) and (6) there is a significant, adimensional parameter k that includes both the information about the supply frequency and of the rotor slip. This parameter can take a series of positive and negative integer values. If the spectrum of the faulty current can be expressed in terms of the harmonic order k, instead of the frequency, then the spectral lines that reveal the presence of the fault can be directly located and evaluated in this new spectrum, termed the harmonic order spectrum, at the positions given by integer values of the harmonic order k. And these positions are the same regardless of the type of supply, the supply frequency, the sampling frequency or the motor load, which greatly facilitates the work of looking for fault signatures in the current spectrum.

In this section, the proposed method will be illustrated using the case of an induction machine with rotor asymmetry. Nevertheless, the same procedure can be followed to the treatment of any other type of machine fault or working conditions.

For the theoretical explanation of HOTA, the stator phase current of a healthy machine will be considered as purely

sinusoidal

$$i_{\rm healthy}(t) = I_{\rm m}\cos(2\pi f_1 t) = I_{\rm m}\cos(\omega_1 t), \tag{7}$$

where $\omega_1 = 2\pi f_1$. In the case of rotor asymmetry, a series of new components associated to the fault appear in the stator current [3]. They can be modelled as an amplitude modulation of the healthy machine's current, with frequencies given by (1),

$$i_{\rm asym}(t) = [1+\beta\cos(2ks\omega_1 t)]\, i_{\rm healthy}(t) \quad k = 1,2,3\ldots. \tag{8}$$

The first step of HOTA is the generation of a rotating current's phasor. Instead of using the three phase currents to build the current's phasor, as in [25], [26], just a single phase current is needed in the proposed method, as in [27].

A rotating current phasor, with variable amplitude and phase

$$\vec{i}_{\rm asym}(t) = A(t)\times e^{j\theta(t)}, \tag{9}$$

can be built so that its projection onto the real axis is precisely the current signal used to build the phasor

$$i_{\rm asym}(t) = \Re\left(\vec{i}_{\rm asym}(t)\right). \tag{10}$$

Among the different possibilities for generating $\vec{i}_{\rm asym}$, there is one of them that is considered as the canonical representation of (9). This canonical representation, known as the analytic signal (AS), is built using the Hilbert transform ($\mathcal{H}$) of the current, as

$$\vec{i}_{\rm asym}(t) = i_{\rm asym}(t) + j\mathcal{H}(i_{\rm asym})(t), \tag{11}$$

where

$$\mathcal{H}(i_{\rm asym})(t) = \frac{1}{\pi}{\rm PV}\int_{-\infty}^{+\infty}\frac{{\rm i}_{\rm asym}(\tau)}{{\rm t}-\tau}{\rm d}\tau. \tag{12}$$

The modulus of the AS, $A(t)$, contains the lower frequencies of the current's signal, and the argument of the AS, $\theta(t)$, contains the higher frequencies.

Under usual working conditions, it can be demonstrated that the current vector (11) has a constant rotating speed ($\frac{d\theta}{dt} = \omega_1$), and a modulus that oscillates with a frequency induced by the asymmetry fault. In effect, assuming that the value of the slip in (8) is low, then the Bedrosian theorem

$$\mathcal{H}(A(\cdot)\times e^{j\theta(\cdot)})(t) = A(t)\times\mathcal{H}(e^{j\theta(\cdot)}) \tag{13}$$

can be applied to (8), giving

$$\mathcal{H}(i_{\rm asym})(t) = [1+\beta\cos(2ks\omega_1 t)]\,\mathcal{H}(i_{\rm healthy})(t). \tag{14}$$

A property of the Hilbert transform is that

$$\mathcal{H}(\cos)(t) = \sin(t), \tag{15}$$

so, applying (15) to (7) and (14) gives

$$\mathcal{H}(i_{\rm asym})(t) = [1+\beta\cos(2ks\omega_1 t)]\, I_{\rm m}\sin(\omega_1 t). \tag{16}$$

Finally, using (11) and (16), the AS of $i_{\rm asym}(t)$ is obtained as

$$\vec{i}_{\rm asym}(t) = [1+\beta\cos(2ks\omega_1 t)]\, I_{\rm m}\times e^{j(\omega_1 t)}, \tag{17}$$

which is a phasor with a constant rotating speed imposed by the supply frequency, ω_1, and a modulus that oscillates with a frequency induced by the asymmetry fault, $2ks\omega_1$.

The second step of HOTA is the expression of the current's phasor $\vec{i}_{\rm asym}$ on a reference frame that rotates synchronously with the rotor. Such a frame can be built by generating a rotating axis in the form

$$\vec{\phi}_{\rm rot}(t) = e^{jp\phi_{\rm rot}(t)}, \tag{18}$$

where $\phi_{\rm rot}(t)$ is the mechanical angular position of the rotor. The rotor position can be obtained by direct measurement, using an absolute or an incremental encoder, or by integration of the measured rotor speed, using a tachometer.

The projection of the current's phasor $\vec{i}_{\rm asym}$ onto this rotating axis, $\vec{i}^{\rm r}_{\rm asym}$, is obtained as

$$\vec{i}^{\rm r}_{\rm asym}(t) = \vec{i}_{\rm asym}(t) * \vec{\phi}_{\rm rot}(t)^*, \tag{19}$$

where the superscript * stands for the complex conjugate.

Assuming steady state regime, (18) can be expressed as

$$\vec{\phi}_{\rm rot}(t) = e^{j(p\omega_{\rm r} t)}, \tag{20}$$

and the slip as

$$s = \frac{\omega_1 - p\omega_{\rm r}}{\omega_1}. \tag{21}$$

Replacing both terms in (17) and (19) gives

$$\vec{i}^{\rm r}_{\rm asym}(t) = [1+\beta\cos(2k(\omega_1 - p\omega_{\rm r})t)]\, I_{\rm m}\times e^{j(\omega_1 - p\omega_{\rm r})t}. \tag{22}$$

In (22), the quantity

$$\omega^{\rm r}_1 = \omega_1 - p\omega_{\rm r} \tag{23}$$

represents the angular speed of the rotating field, imposed by the supply frequency, measured in the rotor's frame. Substituting (23) in (22) gives

$$\vec{i}^{\rm r}_{\rm asym}(t) = [1+\beta\cos(2k\omega^{\rm r}_1)t)]\, I_{\rm m}\times e^{j\omega^{\rm r}_1 t}, \tag{24}$$

and using the cosine expansion

$$\cos(\phi) = \frac{e^{j\phi}+e^{-j\phi}}{2} \tag{25}$$

in (24) gives

$$\vec{i}^{\rm r}_{\rm asym}(t) = I_{\rm m}\times e^{j(\omega^{\rm r}_1)t} + \frac{\beta I_{\rm m}}{2}\times e^{j\omega^{\rm r}_1(1\pm 2k)t)}. \tag{26}$$

The spectral analysis of (26) would reveal the following frequencies, measured in the rotor's frame,

$$\omega^{\rm r}_{\rm asym} = \omega^{\rm r}_1 + 2k\omega^{\rm r}_1 \quad k = 0,\pm1,\pm2,\pm3\ldots, \tag{27}$$

with $\omega^{\rm r}_{\rm asym} = 2\pi f^{\rm r}_{\rm asym}$ and $\omega^{\rm r}_1 = 2\pi f^{\rm r}_1$. Applying a change of scale given by

$$\omega^k = \frac{\omega^r - \omega^{\rm r}_1}{2\omega^{\rm r}_1} \tag{28}$$

to the frequency axis of the spectrum of (26) produces a new spectrum, termed the harmonic order spectrum, where the components generated by the machine's fault appear exactly at the positions given by integer values of the harmonic order,

$$\omega^{\rm k}_{\rm asym} = k \quad k = \pm1,\pm2,\pm3\ldots. \tag{29}$$

Finally, only the amplitudes of the components with integer harmonic order (29) are needed to evaluate the presence of a machine's fault, either by a direct comparison with the thresholds established in the literature, or by performing a trend analysis of the machine's condition during its lifetime. This feature of the proposed method represents a drastic reduction in the number of points that must be stored, analysed and possibly transmitted to perform the diagnostic process, while preserving the diagnostic information contained in the full length spectrum.

Besides, from (26), it can be seen that the amplitude of the captured current signal is not altered in the proposed method, so that the same threshold values used in MCSA to establish the machine's condition can be used unaltered in the proposed HOTA approach.

The proposed method can be summarized as follows:

1) A stator phase current is sampled, and the rotor angular position is measured, either directly (updating the rotor position with the pulses of an encoder, for example), or by integrating the values of a speed sensor.
2) The current's rotating phasor is built using the Hilbert transform of one of the phases' current (11).
3) The rotor position (18) is used to generate a reference frame which rotates synchronously with the rotor.
4) The current's phasor is projected onto the rotor's frame (19).
5) The spectrum of the projected current is computed (27).
6) The frequency axis of this spectrum is re-scaled using (28), so that each harmonic associated to the machine's fault in this harmonic order spectrum appear exactly at an integer harmonic order index (29).
7) The harmonic order spectrum is reduced by keeping only the amplitudes of the components with integer harmonic order. These values can be compared with predefined thresholds to evaluate the machine's condition.

An example of the application of the proposed method can be seen in Fig. 1, which shows the test of an IM, whose characteristics are given in appendix B, working under rated conditions (slip $s = 0.05$), with one broken bar. In the first plot of this figure, Fig. 1.a, the fault can be observed clearly in the spectrum of the stator current: the LSH (2) and the USH (3) appear as sidebands around the supply frequency, at a distance $f_{\text{asym}} = 2\,s\,50 = 5$ Hz. Secondary k order fault components can be observed also in this spectrum, at distances from the supply component given by $2\,k\,s\,50 = 5\,k$ Hz. In Fig. 1.b the spectrum of the current, after having been projected onto the rotor's frame, is shown (step 5 of the proposed method). The supply frequency appears in this spectrum at an absolute value of $f_1^{\text{r}} = s\,50 = 2.5$ Hz. It is remarkable that the dependence of the harmonic frequencies on the motor slip has been eliminated by expressing the stator current phasor in the rotor frame. In this frame, all the fault frequencies appear at odd integer multiples of f_1^{r}, so that a simple shift of this new spectrum by one f_1^{r} interval, and a posterior rescaling in $2f_1^{\text{r}}$ units, (27), produces the harmonic order spectrum, shown in Fig. 1.c (step 6 of the proposed method). Finally, in Fig. 1.d, the reduced harmonic order spectrum

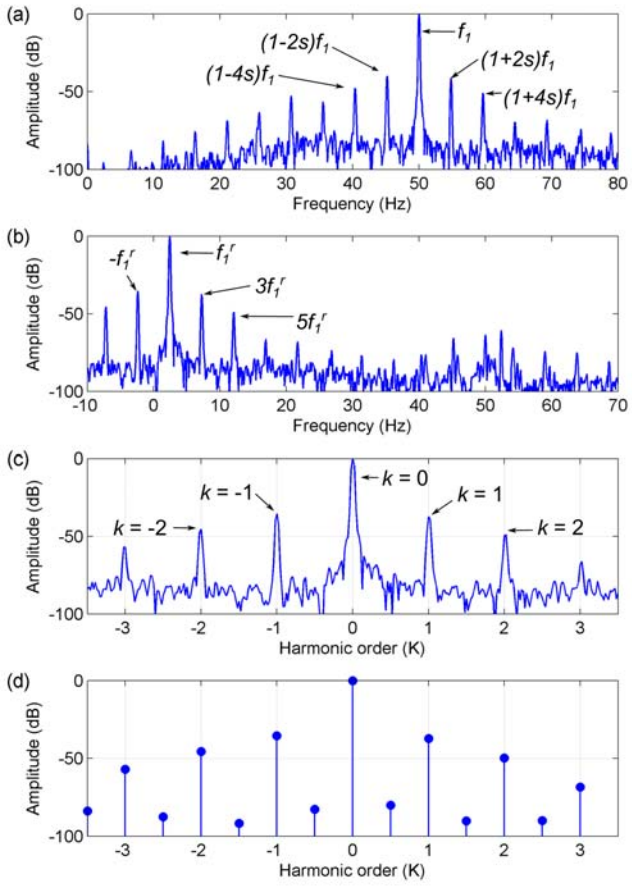

Fig. 1. Example of application of the proposed diagnostic method. (a) Spectrum of the current in the stator frame. (b) Spectrum of the current in the rotor frame. (c) Harmonic order spectrum. (d) Reduced harmonic order spectrum.

is shown. It has been built keeping only the amplitudes of the components of the harmonic order spectrum of Fig. 1.c with integer harmonic order k. Intermediate values have been also included for clarity of the representation. This reduced spectrum (step 7 of the proposed method) has just 15 values, but contains the same information about the fault that the full length spectrum, Fig. 1.a, which has being built using a total number of 10^7 samples. In this way, from a diagnostic point of view, it is only necessary to store, analyse and/or to transmit a small set of 15 values to perform the diagnosis of the machine, irrespectively of the sampling frequency, the supply frequency, the type of supply, the load or the machine condition. This fact facilitates the use of low power/low memory devices and low capacity transmission channels.

III. Experimental validation of the proposed method

The experimental validation of the proposed method has been performed using a commercial induction motor with an artificially forced broken bar, tested under different supply and load conditions. In this section, the test bench is described, and the experimental results obtained are shown and commented. These results highlight one of the strengths of the proposed

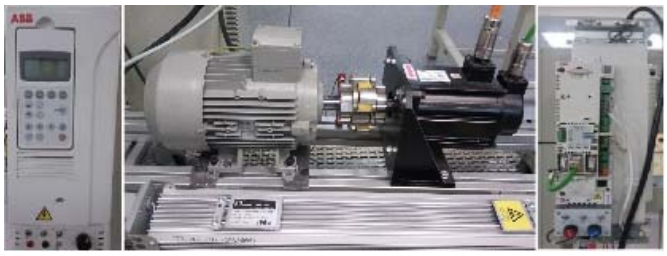

Fig. 2. Test bench. Cage motor coupled to a permanent magnet synchronous machine (center), VSD (left), servo driver (right).

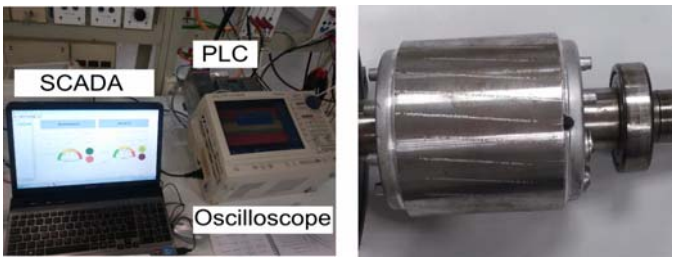

Fig. 3. Test bench control and acquisition system, with PLC, SCADA and oscilloscope (left). Rotor of the tested motor, with a broken bar in the junction with the end ring (right).

approach: its ability to display the diagnostic information about the fault in a very simple and direct way, irrespectively of the supply, load and working conditions of the machine.

A. Test bench

The experimental tests have been carried out using the test bench described in Fig. 2. It allows to fed an IM directly from the mains, or through a variable speed drive (VSD), model ABB ACS800-01-0005-3+E200+L503 (Fig. 2, left). The VSD can be programmed in scalar or direct torque control (DTC) modes. It is equipped with a module (FEN21) which outputs an electronically generated encoder signal with a resolution (programmable) of 720 pulses/revolution. The rotor's angular position, in (18), has been computed with this encoder signal.

A permanent magnet synchronous machine (PMSM) is used as mechanical load. It is controlled by a servodriver, model ABB ACSM1-04AS-024A-4+L516 (Fig. 2, right). The PMSM main characteristics are given in appendix A.

The test bench has been automated using a programmable logic controller (PLC), model ABB PM583 ETH, and a SCADA program (Fig. 3, left). The stator current has been measured using a current clamp (20 A, $0-10$ kHz, 1 A/100 mV, precision class 2). This clamp has been connected to a digital oscilloscope, model Yokogawa DL750, using an analog voltage input module (ref. 701250, 10 Ms, 12 bits). The pulses generated by the VSD electronic encoder unit are sampled with an input module of the oscilloscope (ref. 701280). This equipment is shown in Fig. 3. A sampling rate of 100 kHz has been used, to properly capture the encoder pulses and to avoid the use of anti-aliasing filters, and 100 seconds of the current have been sampled in each test, to be able to resolve the fault harmonics even under no load conditions, giving a total number of 10^7 samples per spectrum.

B. Experimental Tests

An IM, whose characteristics are given in appendix B, has been tested experimentally. A broken bar fault has been produced artificially by drilling a hole in one bar (Fig. 3, right). To cover a wide scenario of working conditions, the following parameters have been changed in different experimental tests:

- The machine condition: healthy or faulty.
- The type of supply. The motor has been fed with direct connection to the mains, and through the VSD. When using the VSD, two control strategies have been tested: scalar control mode, and DTC mode.
- The supply frequency. A 50 Hz supply frequency has been used when the motor is connected to the mains, and lower frequencies have been used when connected to the VSD (25 Hz in scalar control mode and 25.34 Hz in DTC mode).
- The load level. No load, 35% of the rated load, and full rated load have been used to test the viability of the proposed method in the full load range of the motor.

Five different tests (a, b, c, d, and e in Table I) have been performed, with different combinations of these parameters.

TABLE I
EXPERIMENTAL TESTS

	Motor supply	Load level (% rated)	Speed (rpm)	f_1 (Hz)	f_{LSH} (Hz)	f_{USH} (Hz)
(a)	Mains	100 %	2862.2	50	Healthy	Healthy
(b)	Mains	Unloaded	2984.7	50	49.49	50.51
(c)	Mains	100 %	2851.5	50	45.05	54.95
(d)	VSD DTC	Unloaded	1510.8	25.34	25.02	25.66
(e)	VSD scalar	35 %	1442.4	25	23.08	26.92

The first test, for comparison purposes, has been performed with a healthy machine, and the other four tests have been carried out with the machine with a broken bar. Table I also gives the theoretical frequencies of both the LSH (2) and the USH (3) for each test of the faulty machine, whose amplitudes can be compared with predefined thresholds to identify a broken bar fault. As Table I displays, both frequencies must be computed for every working condition of the motor. To perform a reliable diagnosis of the motor, a very precise determination of the supply frequency (which can be measured in the current's spectrum), and of the motor speed (which cannot be obtained from the spectrum), are needed to apply (2) and (3), specially when the motor operates unloaded, or at low speed. Only after the theoretical fault frequencies have been precisely established, the amplitude of the components at these frequencies can be compared with predefined fault thresholds. A slight error in the computation of the position of the fault harmonics (due for example to imprecisions in measuring the speed), can mislead automatic diagnostic systems, and may require the intervention of specialized maintenance personnel. These problems are even worse for higher order harmonics, with $|k| > 1$ in (1), because in this case the errors in the speed measurement are multiplied by the harmonic order.

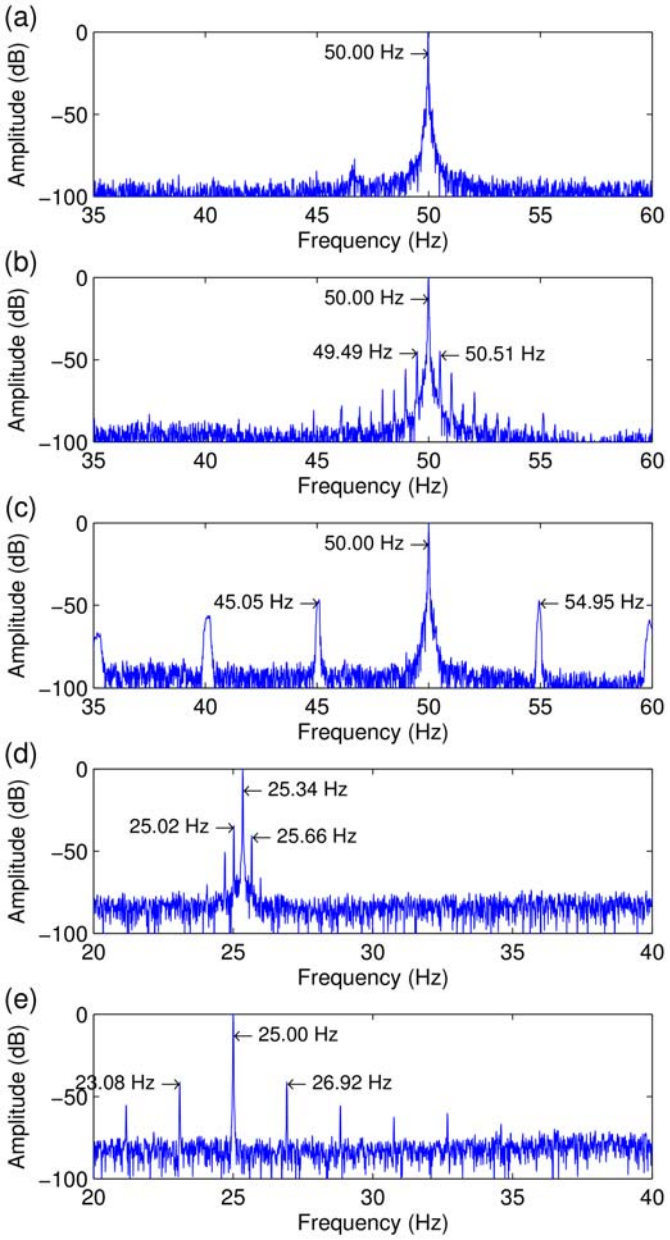

Fig. 4. Spectrum of the current in the five tests of Table I.

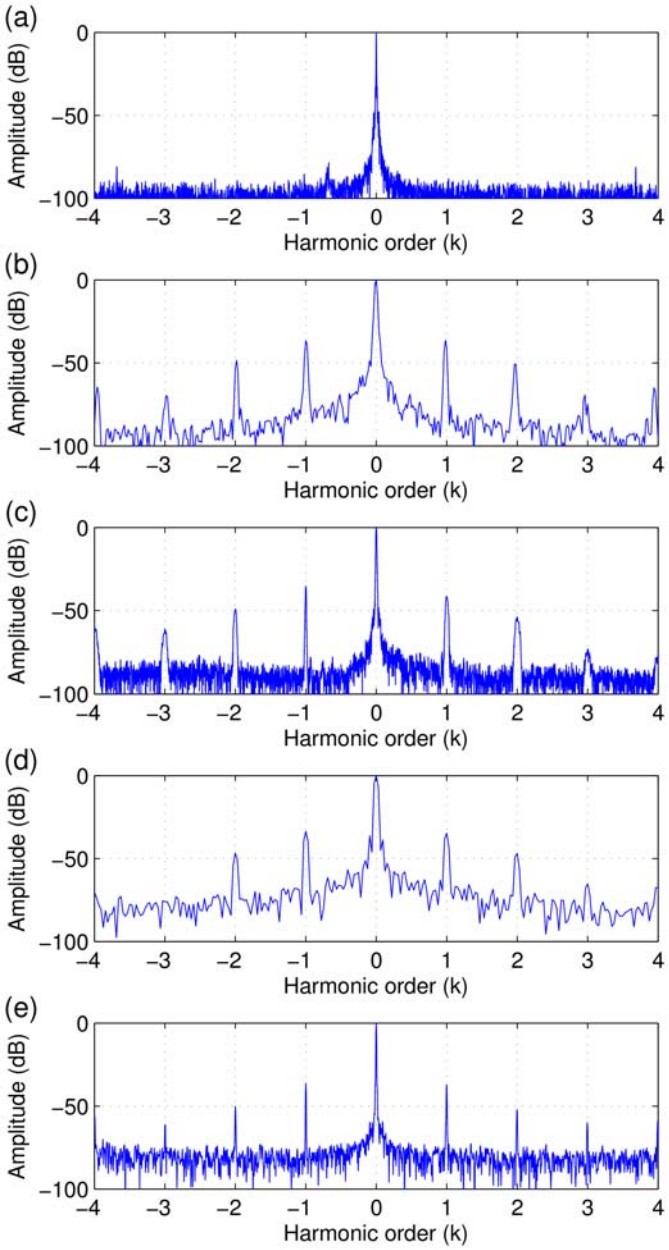

Fig. 5. Harmonic order spectrum of the current in the five tests of Table I.

Traditional MCSA results, using the conventional current spectrum in all the cases covered by Table I, are shown in Fig. 4. As expected, the position of the fault harmonics changes drastically with the motor working conditions. The current spectrum alone cannot be used directly to assess the motor condition, because a subsequent work of computing the position of the fault harmonics must be done to locate their amplitudes in the spectrum.

On the contrary, the harmonic order spectrum, obtained using the proposed method, displays the information about the fault in a clear and extremely simple way, as shown in Fig. 5. In this case, it is not necessary to perform any calculation to locate the fault harmonics in the spectrum, because they appear exactly at integer harmonic order positions. And these positions are the same in the five tests covered by Table I, independently of the working conditions of the motor. Besides, not only the USH and LSH can be identified quickly in the harmonic order spectrum, but also the fault harmonics with higher order numbers, which improves the reliability of the diagnosis.

Additionally, the only values that are needed to assess the motor condition are the amplitudes of the components with integer harmonic order. In this way, the spectrum of Fig. 5 can be reduced to just a few values. This feature is shown in Fig. 6, where just 15 values are kept, while still displaying the presence of a motor fault. The values at intermediate positions between integer harmonic orders have been also kept to improve the legibility of the plots in Fig. 6.

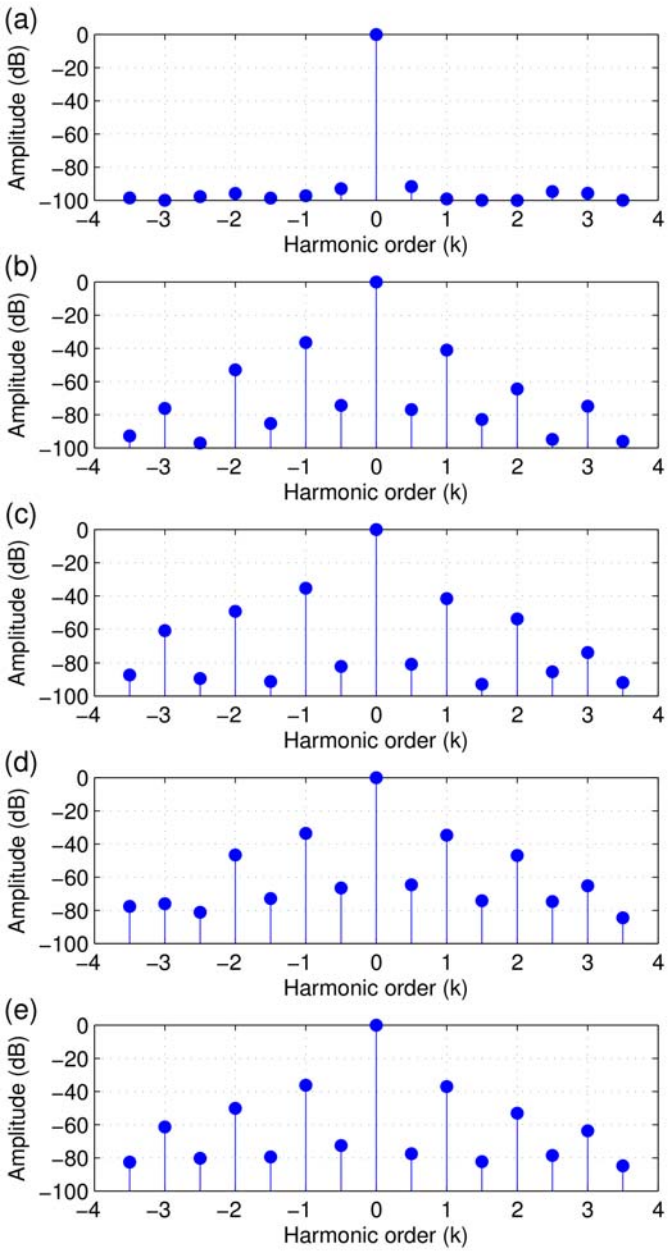

Fig. 6. Reduced harmonic order spectrum of the current in the five tests of Table I.

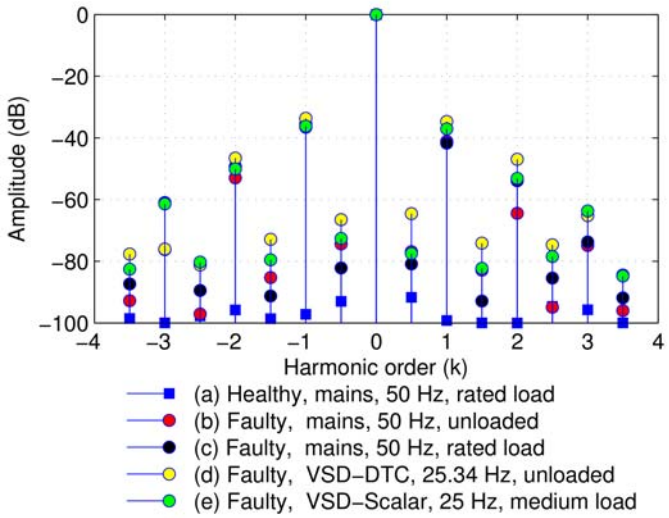

Fig. 7. Superposition in a single plot of the reduced harmonic order spectrum of the current in the five tests of Table I.

Finally, as the harmonic order axis in Fig. 6 is the same for any working condition of the motor, the different plots shown in Fig. 6 can be superimposed in a single plot, as in Fig. 7. This figure shows that the fault information can be identified at the same positions of the harmonic order axis, irrespective of the motor working conditions and supply frequency, which simplifies the spectrum evaluation process in the search of fault signatures.

C. Practical limitations of the proposed approach

The proposed diagnostic approach presents some practical limitations, as in the case of the MCSA approach:

- The slip of the machine, which appears in equations (1) to (6), must be measured accurately. It depends both on the supply's frequency and on the machine's speed. The supply's frequency can be obtained directly from the current's spectrum, but the speed must be acquired with an external sensor, and in certain circumstances (machines with low inertia on shaft, or fed from variable speed drives) there can be errors in the speed measurement. In this case, the fault harmonics appear in a MCSA spectrum at frequencies different from those given by equations (1) to (6), and in the HOTA spectrum at non-integer harmonic orders, but close to them. In such case, the condensed HOTA spectrum is no longer valid, and a full HOTA spectrum must be used for diagnostic purposes. Nevertheless, the proposed approach provides a solution to this problem. Instead of using the speed to compute the rotor's frame position in (18), an encoder can be used, which provides a direct measurement of the rotor position, with an error given by the angular resolution of the encoder, which does not depend on the operating conditions of the machine. In this work, an encoder with 720 pulses per revolution has been used, and the fault harmonics have been obtained at integer orders in the HOTA spectrum in all the tests performed, with a wide range of speed and supply's frequencies.
- In the case of induction machines working at very low slip, as in the case of the experimental tests (b) and (d) of Table I, a high frequency resolution is needed, because the fault harmonics are very close to the supply's component. A long sampling time of 100 seconds has been used in the tests performed in this paper, to achieve a frequency resolution of 0.01 Hz.
- Oscillating mechanical loads, fluctuations of the supply voltage [28], or even the rotor axial ducts [29] may introduce new harmonics in the current's spectrum that, in some cases, appear as false fault harmonics, both in MCSA and HOTA. The use of sidebands around higher order harmonics [28], or the analysis of the current in transient regime [29], [30], among others, have been

proposed to solve this problem. To address this problem, the extension of the HOTA approach to the diagnosis of inductions machines in transient conditions is under development at this moment.

IV. Conclusions

In this paper, a novel approach to the diagnosis of induction machines' faults has been proposed, with a double goal. First, to facilitate the presentation of the fault information in the current spectrum, by directly locating the spectral components generated by the fault at integer harmonic order indexes. And, second, to reduce the amount of spectral values that must be stored, analysed and/or transmitted, to a small set of data points, just the amplitudes of the spectral components with integer harmonic order. With the proposed method, the diagnostic information is displayed exactly at the same positions in the harmonic order spectrum, regardless of the type of supply, the supply frequency, the sampling frequency or the motor load. The description of the proposed method, its theoretical justification, and the experimental validation under a wide variety of supply types and working conditions have been presented in this paper.

The extension of the proposed approach to address the diagnosis of induction motors working in transient conditions, while still keeping the same harmonic order spectrum that has been used in this paper for the steady state regime, is currently under development, and will be presented in a future paper.

Appendix A
Motor Type I

Permanent magnet synchronous machine. Rated characteristics: $P = 4.9$ kW, $f = 50$ Hz, $T = 15.5$ Nm, $I = 14.4$ A , and $n = 3000$ rpm.

Appendix B
Motor Type II

Three-phase induction motor, star connection. Rated characteristics: $P = 1.5$ kW, $f = 50$ Hz, $U = 400$ V, $I = 3.25$ A , $n = 2860$ rpm, and $\cos\varphi = 0.85$.

References

[1] K. Gyftakis and J. Kappatou, "The Zero-Sequence Current as a Generalized Diagnostic Mean in Δ-Connected Three-Phase Induction Motors," *IEEE Trans. Energy Convers.*, vol. 29, no. 1, pp. 138–148, March 2014.

[2] A. Pilloni, A. Pisano, M. Riera-Guasp, R. Puche-Panadero, and M. Pineda-Sanchez, *Fault Detection in Induction Motors.* John Wiley & Sons Ltd, 2013, pp. 275–309.

[3] C. Concari, G. Franceschini, and C. Tassoni, "Induction machine current space vector features to effectively discern and quantify rotor faults and external torque ripple," *Electric Power Applications, IET*, vol. 6, no. 6, pp. 310–321, 2012.

[4] A. Bellini, F. Filippetti, G. Franceschini, C. Tassoni, and G. Kliman, "Quantitative evaluation of induction motor broken bars by means of electrical signature analysis," *IEEE Trans. Ind. Appl.*, vol. 37, no. 5, pp. 1248–1255, 2001.

[5] B. R. Samaga and K. Vittal, "Comprehensive study of mixed eccentricity fault diagnosis in induction motors using signature analysis," *International Journal of Electrical Power & Energy Systems*, vol. 35, no. 1, pp. 180 – 185, 2012.

[6] E. Bouchikhi, V. Choqueuse, and M. Benbouzid, "Current Frequency Spectral Subtraction and Its Contribution to Induction Machines' Bearings Condition Monitoring," *IEEE Trans. Energy Convers.*, vol. 28, no. 1, pp. 135–144, 2013.

[7] X. Gong and W. Qiao, "Bearing Fault Diagnosis for Direct-Drive Wind Turbines via Current-Demodulated Signals," *IEEE Trans. Ind. Electron.*, vol. 60, no. 8, pp. 3419–3428, 2013.

[8] D. Patel and M. Chandorkar, "Modeling and Analysis of Stator Interturn Fault Location Effects on Induction Machines," *IEEE Trans. Ind. Electron.*, vol. 61, no. 9, pp. 4552–4564, Sept 2014.

[9] M. Kaikaa and M. Hadjami, "Effects of the simultaneous presence of static eccentricity and broken rotor bars on the stator current of induction machine," *IEEE Trans. Ind. Electron.*, vol. 61, no. 5, pp. 2452–2463, May 2014.

[10] F. Filippetti and M. Artioli, "Simple ideas for light but robust signal processing of electromechanical systems," in *IECON 02 [Industrial Electronics Society, IEEE 2002 28th Annual Conference of the]*, vol. 4, 2002, pp. 3366–3371.

[11] L. Hou and N. Bergmann, "Novel Industrial Wireless Sensor Networks for Machine Condition Monitoring and Fault Diagnosis," *IEEE Trans. Instrum. Meas.*, vol. 61, no. 10, pp. 2787–2798, 2012.

[12] D. Matic, F. Kulic, M. Pineda-Sanchez, and I. Kamenko, "Support vector machine classifier for diagnosis in electrical machines: Application to broken bar," *Expert Systems with Applications*, vol. 39, no. 10, pp. 8681–8689, 2012.

[13] R. Romero-Troncoso, R. Saucedo-Gallaga, E. Cabal-Yepez, A. Garcia-Perez, R. Osornio-Rios, R. Alvarez-Salas, H. Miranda-Vidales, and N. Huber, "FPGA-Based Online Detection of Multiple Combined Faults in Induction Motors Through Information Entropy and Fuzzy Inference," *IEEE Trans. Ind. Electron.*, vol. 58, no. 11, pp. 5263–5270, 2011.

[14] J. Urresty, J.-R. Riba Ruiz, and L. Romeral, "Diagnosis of interturn faults in pmsms operating under nonstationary conditions by applying order tracking filtering," *IEEE Trans. Power Electron.*, vol. 28, no. 1, pp. 507–515, 2013.

[15] M. Akar, "Detection of a static eccentricity fault in a closed loop driven induction motor by using the angular domain order tracking analysis method," *Mechanical Systems and Signal Processing*, vol. 34, no. 12, pp. 173–182, 2013.

[16] Z. Fu, D. Brown, and B. Haynes, "A new method of non-stationary signal analysis for control motor bearing fault diagnosis," in *Intelligent Signal Processing, 2003 IEEE International Symposium on*, 2003, pp. 99–104.

[17] C. Wolf and R. Lorenz, "Using the motor drive as a sensor to extract spatially dependent information for motion control applications," *IEEE Trans. Ind. Appl.*, vol. 47, no. 3, pp. 1344–1351, 2011.

[18] A. Lebaroud and A. Medoued, "Online computational tools dedicated to the detection of induction machine faults," *International Journal of Electrical Power & Energy Systems*, vol. 44, no. 1, pp. 752 – 757, 2013.

[19] L. Saidi, F. Fnaiech, H. Henao, G. Capolino, and G. Cirrincione, "Diagnosis of broken-bars fault in induction machines using higher order spectral analysis," *ISA Transactions*, vol. 52, no. 1, pp. 140–148, 2013.

[20] S. Choi, B. Akin, M. Rahimian, and H. Toliyat, "Implementation of a Fault-Diagnosis Algorithm for Induction Machines Based on Advanced Digital-Signal-Processing Techniques," *IEEE Trans. Ind. Electron.*, vol. 58, no. 3, pp. 937–948, 2011.

[21] M. Cabanas, F. Pedrayes, C. Rojas, M. Melero, J. Norniella, G. Orcajo, J. Cano, F. Nuno, and D. Fuentes, "A New Portable, Self-Powered, and Wireless Instrument for the Early Detection of Broken Rotor Bars in Induction Motors," *IEEE Trans. Ind. Electron.*, vol. 58, no. 10, pp. 4917–4930, 2011.

[22] K. Shahzad, P. Cheng, and B. Oelmann, "Architecture Exploration for a High-Performance and Low-Power Wireless Vibration Analyzer," *IEEE Sensors J.*, vol. 13, no. 2, pp. 670–682, 2013.

[23] P. Vaclavek, P. Blaha, and I. Herman, "AC Drive Observability Analysis," *IEEE Trans. Ind. Electron.*, vol. 60, no. 8, pp. 3047–3059, 2013.

[24] D. J. White, P. E. William, M. W. Hoffman, and S. Balkir, "Low-Power Analog Processing for Sensing Applications: Low-Frequency Harmonic Signal Classification," *Sensors*, vol. 13, no. 8, pp. 9604–9623, 2013.

[25] B. Akin, S. Choi, U. Orguner, and H. Toliyat, "A Simple Real-Time Fault Signature Monitoring Tool for Motor-Drive-Embedded Fault Diagnosis Systems," *IEEE Trans. Ind. Electron.*, vol. 58, no. 5, pp. 1990–2001, 2011.

[26] C. Concari, G. Franceschini, C. Tassoni, and A. Toscani, "Validation of a faulted rotor induction machine model with an insightful geometrical interpretation of physical quantities," *IEEE Trans. Ind. Electron.*, vol. 60, no. 9, pp. 4074–4083, 2013.

[27] R. Puche-Panadero, M. Pineda-Sanchez, M. Riera-Guasp, J. Roger-Folch, E. Hurtado-Perez, and J. Perez-Cruz, "Improved Resolution of the MCSA Method Via Hilbert Transform, Enabling the Diagnosis of Rotor Asymmetries at Very Low Slip," *IEEE Trans. Energy Convers.*, vol. 24, no. 1, pp. 52–59, 2009.
[28] C. Pezzani, P. Donolo, G. Bossio, M. Donolo, A. Guzman, and S. Zocholl, "Detecting Broken Rotor Bars With Zero-Setting Protection," *IEEE Trans. Ind. Appl.*, vol. 50, no. 2, pp. 1373–1384, March 2014.
[29] C. Yang, T. Kang, D. Hyun, S. Lee, J. Antonino-Daviu, and J. Pons-Llinares, "Detection of induction motor rotor faults under the rotor axial air duct influence," *IEEE Trans. Ind. Appl.*, in press.
[30] F. Vedreno-Santos, M. Riera-Guasp, H. Henao, M. Pineda-Sanchez, and R. Puche-Panadero, "Diagnosis of rotor and stator asymmetries in wound-rotor induction machines under nonstationary operation through the instantaneous frequency," *IEEE Trans. Ind. Electron.*, vol. 61, no. 9, pp. 4947–4959, Sept 2014.

Angel Sapena-Baño obtained its M.Sc. degree in Electrical Engineering in 2008 from the Universitat Politècnica de València (Spain). From 2008 he works as a Researcher in the Institute for Energy Engineering of Universitat Politècnica de València. His research interests focus on induction motor diagnostics and the maintenance based on the condition monitoring, numerical modelling of electrical machines, and advanced automation processes and electrical installations.

Juan Perez-Cruz (M09) obtained his M.Sc. degree in 1997 and his Ph.D. degree in 2006 from the Universitat Politècnica de València, both in Electrical Engineering. From 1970 to 1992 he worked in the electrical industry in the field of industrial systems maintenance and automation. In 1992 he joined the Universitat Politècnica de València and is currently Associate Professor of electrical installations and machines. His research interests focus on induction motor diagnostics, numerical modelling, and automation.

Manuel Pineda-Sanchez (M02) received his M.Sc. degree in 1985 and his Ph.D. degree in 2004 from the Universitat Politècnica de València, both in Electrical Engineering. Currently he is an Associate Professor in the Department of Electrical Engineering of the Universitat Politècnica de València. His research interests include electrical machines and drives, induction motor diagnostics, and numerical simulation of electromagnetic fields.

Ruben Puche-Panadero (M09) received his M.Sc. degree in Automatic and Electronic Engineering in 2003, and its Ph.D. degree in Electrical Engineering in 2008, both from the Universitat Politècnica de València. He joined the Universitat Politècnica de València in 2006 and he is currently Associate Professor of Control of Electrical Machines. His research interests focus on induction motor diagnosis, numerical modeling of electrical machines, and advanced automation processes and electrical installations.

Jose Roger-Folch (M03) received the M.Sc. degree from the Universidad Politecnica de Catalua, Barcelona, Spain, in 1970, and the Ph.D. degree from the Universitat Politècnica de València, Spain, in 1980, both in Electrical Engineering. From 1971 to 1978, he worked in the electrical industry as a Project Engineer. Since 1978, he has been with the Department of Electrical Engineering, Universitat Politècnica de València, where he is currently a Professor of Electrical Installations and Machines. His main research areas are numerical methods applied to the design and maintenance of electrical machines and equipment.

Martin Riera-Guasp (M94-SM12) received the M.Sc. degree in Industrial Engineering and the Ph.D. degree in Electrical Engineering from the Universitat Politècnica de València (Spain) in 1981 and 1987, respectively. Currently he is an Associate Professor in the Department of Electrical Engineering of the Universitat Politècnica de València. His research interests include condition monitoring of electrical machines and electrical systems efficiency.

Javier Martnez-Romn was born in 1965. He received the Ph.D. degree in Electrical Engineering from the Universitat Politècnica de València, Spain, in 2002. Currently he is Associate Professor with the Universitat Politècnica de València. His primary areas of interest are electrical machines and drives. Dr. Martnez-Romn has participated in various international projects supported by the European Union. He has published several papers on electrical machines in international journals and conference proceedings.